Hindawi
Scientific Programming
Volume 2022, Article ID 6117804, 11 pages
https://doi.org/10.1155/2022/6117804

Research Article

Analysis of the Coupling and Coordination Relationship between the Evolution of Enterprise Spatial Structure and Economic Development Based on the Deep Learning Model

Lei Wang,[1] Yuan He,[2] and Yao Qi[3]

[1]*School of Economics and Management, Jiaozuo Normal College, Jiaozuo 454000, China*
[2]*Department of Finance and Business, Henan College of Industry & Information Technology, Jiaozuo 454000, China*
[3]*School of Business Administration, Henan Polytechnic University, Jiaozuo 454000, China*

Correspondence should be addressed to Yao Qi; qiyao@hpu.edu.cn

Received 4 January 2022; Revised 24 January 2022; Accepted 16 February 2022; Published 18 March 2022

Academic Editor: Hangjun Che

This study is based on the unsupervised learning-based enterprise spatial structure evolution and economic coupling coordination relationship situation assessment method. Pattern recognition has high-precision characteristics, but it is necessary to train the evaluation model for the enterprise spatial structure evolution in advance and then carry out economic coupling coordination based on the trained model. The conclusions are as follows: (1) through the RC1, RC2, RC3, RC4, RC5, and RC6 evaluation indicators to evaluate the situation evaluation method based on the unsupervised learning of the evolution of the enterprise spatial structure and the economic coupling and coordination relationship, it is found that the main component characteristics as a whole meet the standard. The optimal RC is RC6: profit = −0.0885, highest = −0.0809, lowest = −0.0932, WR.WR2 = 0.0038, MA.MA3 = −0.0782, MTM.MTM = −0.0427, OSC.OSC = −0.0355, ROC.MAROC = 0.0105, SKDJ.D = −0.0268, BIAS-QL.BIAS = −0.01, WIDTH.WIDTH = 0.2408, CYD.CYDN = −0.0961, FSL.SWL = −0.0868ADTM.ADTM = −0.0379, ATR.ATR = −0.0278, DMA.DIFMA = −0.0358, DMI.ADX = 0.8516, DMI.ADXR = 0.854, EMV.EMV = −0.0942, VMACD.DIF = 0.3312, and UOS.MAUOS = −0.0846.2. Based on the deep learning model of the coupling and coordination relationship between the evolution of the spatial structure of the enterprise, the time-dependent matrix comparison experiment is divided into directed + self, directed, undirected + self, and undirected time for comparison. The experimental results on directed + self are the best; with various indicators, the upward improvement is above 10%: CP = 0.8611, CR = 0.9353, C–F1 = 0.8967, EP = 0.8865, ER = 0.857, E–F1 = 0.917, OP = 0.856, OR = 0.9845, and O–F1 = 0.99.3. The time cost, profit, and transaction volume data of the company are collected for a certain period of time, and simulation experiments are conducted to get a small difference between the predicted result and the actual data. The January data are closest to the true value: cost = 30.78, profit = 30.11, highest = 30.1, lowest = 29.7, WR.WR1 = 81.21, WR.WR2 = 45.62, AMV.AMV2 = 32.67, AMV.AMV3 = 34.95, and MCST. MCST = 36.08.4. In the model score, the best performance of LSTM data is CP = 0.3829, CR = 0.3664, C–F1 = 0.3744, EP = 0.3726, ER = 0.3004, E–F1 = 0.3326, OP = 0.9155, OR = 0.9316, and O–F1 = 0.9234, which is better than the BiLSTM model with CP = 0.3648, CR = 0.3319, C–F1 = 0.3392, EP = 0.4402, ER = 0.391, E–F1 = 0.4145, OP = 0.9215, OR = 0.9318, and O–F1 = 0.9266.

1. Introduction

Deep learning (DL) network, also known as deep neural network, derived from the artificial neural network, simulates the human brain to learn and perceive the outside world, and its core neurons are a new field in machine learning research. Both deep learning and shallow learning methods simulate the human brain to perceive the outside world. The difference between the two is that the deep learning model can transform high-dimensional complex feature data into higher levels and more through deep and simple linear and nonlinear network structures. Abstract representation was used to carry out deep learning algorithms such as deep self-encoding networks. It has good

characterization ability for high-dimensional complex deep self-encoding network [1–3]. Deep self-encoding networks can have outstanding advantages in processing large-scale, nonlinear, and multidimensional data. The gated recurrent unit neural network in the rise of deep neural networks has the function of data security situation assessment and is suitable for processing deep neural network time series data. Generative adversarial network (GAN) has a good effect in the field of intelligent robot data generation under wireless connection. Based on deep learning, an adaptive feature quantitative evaluation method of intelligent robot clusters based on convolutional neural network (CNN) under wireless connection has emerged. This method combines the coupling and coordination relationship of the evolution of enterprise spatial structure with the characteristics of CNN and realizes a comprehensive quantitative evaluation of deep neural networks through self-adaptive deep self-encoding features such as online learning. Artificial intelligence researchers use neural networks as a way to express complex problems in a nonlinear way. In recent years, they have been applied in the field of biological theory and artificial intelligence. The research of neuron perceptron has received extensive attention [4–6]. Deep neural networks are derived from neural networks and are superior to traditional neuron perceptron networks. Artificial intelligence research using deep neural networks will be a very promising research direction. Artificial intelligence researchers have designed the neuron unit in the artificial neural network in the deep self-encoding network, also known as the high-dimensional complex deep self-encoding network perceptron, which receives the information input of the high-dimensional complex deep network and after time series data processing outputs the result. Since the human body's perception of the external world is realized by interconnecting deep autoencoding networks formed by hundreds of neurons, the artificial neural network designs perceptrons of high-dimensional complex deep autoencoding networks to connect them to each other. According to the high-dimensional complex deep self-encoding network signal processing flow, it is divided into a data security input layer, a time series hidden layer, and a self-encoding network output layer. The perceptron layer that initially senses the incoming signal is called the input layer [5–9]. The perceptron layer that processes internal signals and continues to output internal signals is called the hidden layer, and the signal that is responsible for the final output of the relationship between the evolution of the enterprise's spatial structure and the economic coupling is called the output layer. Deep neural network, as an extension of artificial neural network vector machine and feature gravity search algorithm, adds more vector machine feature search on its basis. The neurons in the data security input layer, the time series hidden layer, and the output layer of the self-encoding network are fully connected. As the number of output layers of the self-encoding network increases, deep neural networks have stronger learning output capabilities. In order to solve the parameter selection problem of deep self-encoding network and high-dimensional complex deep self-encoding network in machine learning technology, support vector machine and feature gravity search algorithm (GSA) can be combined based on parameter optimization, so that the neural network security situation assessment system has better global optimization function. A cyberspace method based on an improved feature gravity search algorithm can be optimized using high-dimensional complex deep self-encoding network learning strategies and simulation methods, which significantly improves the accuracy of the feature gravity search algorithm and the computational efficiency of the cyberspace method. The neural network method that optimizes the network space method of the feature gravity search algorithm can be used to perform an adaptive mechanism of neural network training efficiency through the cuckoo neural network algorithm. In this paper, the method of sequential data processing based on conjugate gradient is introduced [10–13].

With the development of machine learning technology, pattern recognition methods such as deep autoencoding networks, high-dimensional complex deep autoencoding networks, data security situation assessment functions, and time series data vector machines have also been widely used in the coordination of the evolution of enterprise spatial structure and economic coupling. Based on the characteristics of deep autoencoder (DAE) and deep neural network (DNN) [14, 15], a method for analyzing the relationship between the evolution of enterprise spatial structure and economic coupling is proposed, which improves the accuracy of identifying the evolution of the enterprise's spatial structure and the flexibility of the relationship between economic coupling and coordination. On the basis of the traditional hierarchical model, unsupervised learning is performed by using neurons to perceive signal data through synapses, combined with a variational autoencoder (VAE) to process new output signals. Finally, a method for evaluating the situation of the coordination relationship between the evolution of the spatial structure of the enterprise and the economic coupling based on unsupervised learning is formed. Pattern recognition based on unsupervised learning-based enterprise spatial structure evolution and economic coupling coordination relationship situation assessment method has high-precision characteristics, but it is necessary to train the evaluation model for the enterprise spatial structure evolution in advance and then carry out economic coupling coordination based on the trained model.

2. Evolution of Enterprise Spatial Structure and Economic Development

2.1. Deep Learning Model. The deep learning model is a network model that is further developed on the basis of deep neural networks. It can greatly reduce the number of parameters through weight sharing. At the same time, convolutional neural networks can process multidimensional input data of the evolution of the enterprise's spatial structure and the coordination relationship between economic coupling and retention. The original local spatial information of the input data of the deep self-encoding network in the machine learning technology has been greatly

improved, and its feature extraction ability has also been greatly improved. It is mainly used in the processing of enterprise spatial structure evolution and economic coupling recognition. The nodes between the various convolutional neural layers of the deep learning model are connected to each other to make it have the memory function of the network model. It can obtain the hidden layer state of the spatial structure evolution and then calculate the output of the hidden layer at the current time according to the output of the input layer at the current time. It solves the problem that the fully connected deep neural network cannot model time series data. It is mainly used to deal with the evolution of the enterprise spatial structure and the identification of economic coupling. The deep learning model is shown in Figure 1 [16–18].

2.2. Coupling and Coordination Relationship of the Evolution of Enterprise Spatial Structure Based on the Deep Learning Model. The deep learning model-based corporate spatial structure evolution coupling coordination relationship model includes corporate structure filtering algorithms, as well as deep learning model resource recommendation and resource display algorithms. Therefore, it is necessary to design the algorithms required for the coupling and coordination relationship model of the evolution of the enterprise space structure, and at the same time, through experiments, adjust the parameters of the deep learning models designed by different companies, select better parameters, and finally coordinate the relationship through the evolution of the enterprise space structure. The real dataset is compared with the classic algorithm to verify the feasibility and rationality of the designed algorithm. The coupling and coordination relationship model of the evolution of the enterprise spatial structure includes the data layer, the evaluation layer, and the knowledge layer, as shown in Figure 2. The evolution of the spatial structure of an enterprise cannot be done without the support of big data for the development of the coupling and coordination relationship, and big data cannot do it without the deep learning model technology. Therefore, data processing technology plays an important role in resource recommendation and resource display algorithms. Datasets usually need to be preprocessed [19]. Especially for the dataset in the field of enterprise spatial structure, preprocessing the dataset can filter out the impurity information of the evolution of the silent structure of the enterprise to a certain extent.

2.3. Data Processing Technology. Data processing refers to the evolution of the enterprise's spatial structure, coupling and coordinating relational data acquisition, data cleaning, data processing, and data visualization. The significance of data processing is to transform the company's messy data source processing into information useful for deep learning model resource recommendation and resource display algorithms. The filtering algorithm deletes outlier data and duplicate data and normalizes and standardizes the data, so that we can store, search, analyze, and reuse the outlier data and duplicate data. Data processing technology is the deep learning technology to realize the automation of data processing. Instead of manual work, it can relatively easily process the evolution of the enterprise's spatial structure, coupling and coordinating relational data, effectively saving the cost and time of data processing. For large-scale enterprise spatial structure evolution, coupling and coordinating relational data processing are quite complicated, and it is difficult to complete it manually. Therefore, corresponding tools or technical means are needed to complete data processing tasks.

3. Application of the Deep Learning Model in Enterprise Economic Development

3.1. LSTM [20–22].

$$X = \{x_1, x_2 \dots x_n\}. \tag{1}$$

The deep learning model is defined as follows:

$$\begin{aligned} h_t &= f(Ux_t + Wh_{t-1}), \\ o_t &= g(Vh_t). \end{aligned} \tag{2}$$

The number of parameters is defined as follows:

$$o_t = g(Vf(Ux_t + Wh_{t-1})). \tag{3}$$

3.1.1. Analysis on the Coordination Relationship between the Evolution of Enterprise Spatial Structure and Economic Coupling.

$$\begin{aligned} o_t &= g(Vf(UX_t + Wf(Ux_{t-1} + Wh_{t-2}))), \\ z_t &= \sigma(W_z \cdot [h_{t-1}, x_t]), \\ r_t &= \sigma(W_r \cdot [h_{t-1}, x_t]). \end{aligned} \tag{4}$$

Input data are defined as follows:

$$\begin{aligned} h' &= \tanh(W \cdot [r_t * h_{t-1}, x_t], \\ h_t &= (1 - z_t) * h_{t-1} + z_t * h_t', \\ Z^{l+1}(i, j) &= \left[Z^l \otimes w^{l+1}\right](i, j) + b. \end{aligned} \tag{5}$$

3.2. BiLSTM [23].

$$Z^{l+1}(i, j) = \sum_{k=1}^{kl} \sum_{x=1}^{f} \sum_{y=1}^{f} [Z_k^l(s_o i + x, s_o j + y) + b. \tag{6}$$

Machine learning technology is defined as follows:

$$\begin{aligned} (i, j) &\in \{0, 1, \dots, L_{l+1}\}, L_{l+1} = \frac{L_l + 2p - f}{s_o}, \\ g_v &= \mathrm{ReLU}\left(\sum_{u \in N(v)} h_u \cdot W_{L(u,v)}\right), \\ E &= -\sum_{i=0}^{n} X_i \log P(X_i). \end{aligned} \tag{7}$$

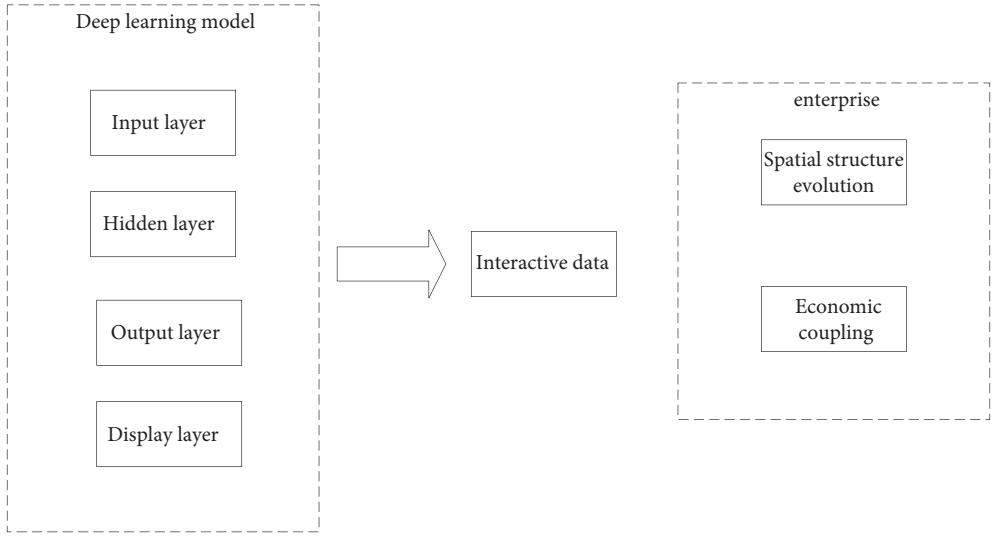

Figure 1: Deep learning model.

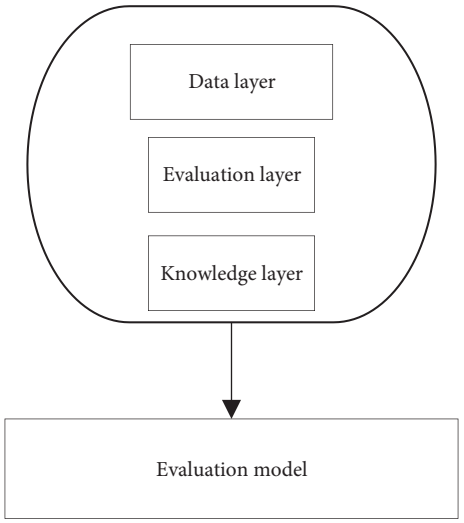

Figure 2: Coupling and coordination relationship model for the evolution of enterprise spatial structure.

Deep autoencoding network is defined as follows:

$$\begin{aligned} E &= -\sum_{i=0}^{2} X_i \log\, P(X_i), \\ \widehat{\beta} &= \arg\min_{\beta \in R^d}, \\ \beta &= \arg\min_{\beta \in R^d} \|Y - X\beta\|^2 \text{ s.t.}, \\ &\sum_{j=1}^{d} \left|\beta_j\right| \le t, \quad t \ge 0. \end{aligned} \tag{8}$$

Enterprise spatial structure evolution is defined as follows:

$$\begin{aligned} \beta &= \arg\min_{\beta \in R^d} \left(\|Y - X\beta\|^2 + \lambda \sum_{j=1}^{d} \left|\beta_j\right|, \right. \\ t_0 &= \sum_{j=1}^{d} \left|\beta_j\,(\mathrm{OLS})\right|. \end{aligned} \tag{9}$$

3.3. GCN [15, 24–26].

$$X = \left(X_1, X_2, X_3, \ldots, X_p\right)^T,$$
$$Z_{ij} = \frac{x_{ij} - \overline{x}_j}{s_j}. \tag{10}$$

3.3.1. Analysis on the Coupling and Coordination Relationship of Enterprise Economy.

$$i = 1, 2, \ldots, n,$$
$$j = 1, 2, \ldots, p. \tag{11}$$

3.3.2. The Evolution of Enterprise Spatial Structure Based on the Deep Learning Model.

$$\overline{x}_j = \frac{\sum_{i-1}^{n} x_{ij}}{n},$$
$$s_j^2 = \frac{\sum_{i-1}^{n}\left(x_{ij} - \overline{x}_j\right)^2}{n-1}. \tag{12}$$

Financial analysis is defined as follows:

$$R = \left[r_{ij}\right]_p xp = \frac{Z^t Z}{n - 1^r},$$
$$U_{ij} = z_i^T b_j^o, \quad j = 1, 2, \ldots, m. \tag{13}$$

4. Simulation Experiment

4.1. Principal Component Feature Analysis. RC1, RC2, RC3, RC4, RC5, and RC6 are used to evaluate the situation evaluation method based on the unsupervised learning of the evolution of the spatial structure of the enterprise and the economic coupling and coordination relationship, and it is found that the main component characteristics as a whole meet the standard. The optimal RC is RC6: profit = −0.0885, highest = −0.0809, lowest = −0.0932, WR.WR2 = 0.0038, MA.MA3 = −0.0782, MTM.MTM = −0.0427, OSC.OSC = −0.0355, ROC.MAROC = 0.0105, SKDJ.D = −0.0268, BIAS-QL.BIAS = −0.01, WIDTH.WIDTH = 0.2408, CYD. CYDN = −0.0961, FSL.SWL = −0.0868, ADTM.ADTM = −0.0379, ATR.ATR = −0.0278, DMA.DIFMA = −0.0358, DMI.ADX = 0.8516, DMI.ADXR = 0.854, EMV.EMV = −0.0942, VMACD.DIF = 0.3312, and UOS.MAUOS = −0.0846, as shown in Table 1 and Figure 3.

4.2. Evaluation Indicators for the Coupling and Coordination Relationship of the Evolution of Enterprise Spatial Structure Based on the Deep Learning Model. Based on the deep learning model of the enterprise spatial structure evolution coupling and coordination relationship model, the principal component evaluation index algorithm is included. It is necessary to design the principal component evaluation indicators of the enterprise spatial structure evolution coupling coordination relationship model and, at the same time, through experiments, to design the principal components of different companies. The evaluation index is adjusted, and finally the principal component evaluation index is obtained through the coupling and coordination relationship of the evolution of the enterprise's spatial structure. Indicators CP, CR, C–F1, EP, ER, E–F1, OP, OR, O–F1, PCNT.PCNT, PCNT.MAPCNT, AMO.AMO2, VRSI.RSI3, AMV.AMV2, AMV.AMV3, and MCST.MCST are used to evaluate the model. It is found that, in the coupling and coordination relationship of the evolution of enterprise spatial structure based on the deep learning model, when RC = 6, the indicators are optimal: CP = −0.0184, CR = −0.0933, C–F1 = −0.3346, EP = −0.0051, ER = 0.1221, E–F1 = 0.0195, OP = −0.5153, OR = 0.1523, O–F1 = −0.113, PCNT.PCNT = −0.0023, PCNT.MAPCNT = −0.018, AMO.AMO2 = −0.022, VRSI.RSI3 = 0.2018, AMV.AMV2 = −0.076, AMV.AMV3 = −0.0543, and MCST.MCST = 0.0148, as shown in Table 2 and Figure 4.

4.3. Time-Dependent Matrix Comparison Experiment. Based on the deep learning model of enterprise spatial structure evolution coupling coordination relationship model, the time-dependent matrix comparison experiment is divided into directed + self, directed, undirected + self, and undirected time for comparison. The experimental result on directed + self is the most effective. The indicators are improved by more than 10%: CP = 0.8611, CR = 0.9353, C–F1 = 0.8967, EP = 0.8865, ER = 0.857, E–F1 = 0.917, OP = 0.856, OR = 0.9845, and O–F1 = 0.99, as shown in Table 3 and Figure 5.

4.4. Simulation Experiments in Different Companies. The time cost, profit, and transaction volume data of the company are collected for a certain period of time, and simulation experiments are conducted to get a small difference between the predicted result and the actual data. The January data are closest to the true value: cost = 30.78, profit = 30.11, highest = 30.1, lowest = 29.7, WR.WR1 = 81.21, WR.WR2 = 45.62, AMV.AMV2 = 32.67, AMV.AMV3 = 34.95, and MCST. MCST = 36.08, as shown in Table 4 and Figure 6.

Then, different models are compared to predict the economic development of the company. In the LSTM model, A company = −1.03, B company = −0.9, C company = −0.95, D company = −0.94, E company = −0.96, F company = −0.68, G company = −0.67, H company = −0.59, I company = −0.49, and J company = −0.56. The LSTM model is obtained as the optimal model, as shown in Table 5 and Figure 7.

4.5. Scoring of Different Models. The scoring standards include accuracy (P), recall (R), and F1 scoring experiment results. The best performance of LSTM data is CP = 0.3829, CR = 0.3664, C–F1 = 0.3744, EP = 0.3726, ER = 0.3004, E–F1 = 0.3326, OP = 0.9155, OR = 0.9316, and O–F1 = 0.9234, which is better than the BiLSTM model with CP = 0.3648, CR = 0.3319, C–F1 = 0.3392, EP = 0.4402,

Table 1: Principal component analysis.

	RC1	RC2	RC3	RC4	RC5	RC6
Profit	0.9452	0.195	0.2122	0.0049	−0.0289	−0.0885
Highest	0.9448	0.1982	0.2196	0.058	−0.006	−0.0809
Lowest	0.9413	0.1962	0.2103	0.0511	−0.0609	−0.0932
WR.WR2	−0.001	−0.2737	0.0275	−0.0395	0.0512	0.0038
MA.MA3	0.9734	−0.1121	0.1559	−0.0541	−0.0241	−0.0782
MTM.MTM	−0.0032	0.8769	0.1252	0.2854	−0.0061	−0.0427
OSC.OSC	−0.0011	0.8331	0.1869	0.4332	−0.0202	−0.0355
ROC.MAROC	0.0338	0.8914	0.3031	−0.0275	0.0344	0.0105
SKDJ.D	0.0389	0.8678	0.0432	0.106	−0.0683	−0.0268
BIAS-QL.BIAS	−0.0362	0.3561	0.0002	0.8862	−0.0239	−0.01
WIDTH.WIDTH	0.1058	0.014	0.021	0.0285	0.7291	0.2408
CYD.CYDN	0.1315	0.3727	0.2886	0.3361	−0.5788	−0.0961
FSL.SWL	0.9611	0.1197	0.215	−0.0159	−0.0272	−0.0868
ADTM.ADTM	0.0591	0.5492	0.6507	0.0818	−0.1677	−0.0379
ATR.ATR	0.6541	−0.0014	0.2166	0.0058	0.5668	−0.0278
DMA.DIFMA	0.2072	0.098	0.8759	−0.0667	0.0374	−0.0358
DMI.ADX	−0.0985	−0.0335	0.008	−0.0152	0.1862	0.8516
DMI.ADXR	−0.1379	−0.0591	0.0294	0.0072	0.2531	0.854
EMV.EMV	0.0275	0.8208	0.2628	0.1308	−0.0963	−0.0942
VMACD.DIF	−0.0466	0.6583	0.1273	0.1629	0.113	0.3312
UOS.MAUOS	0.0941	0.8208	0.2045	0.1164	0.027	−0.0846

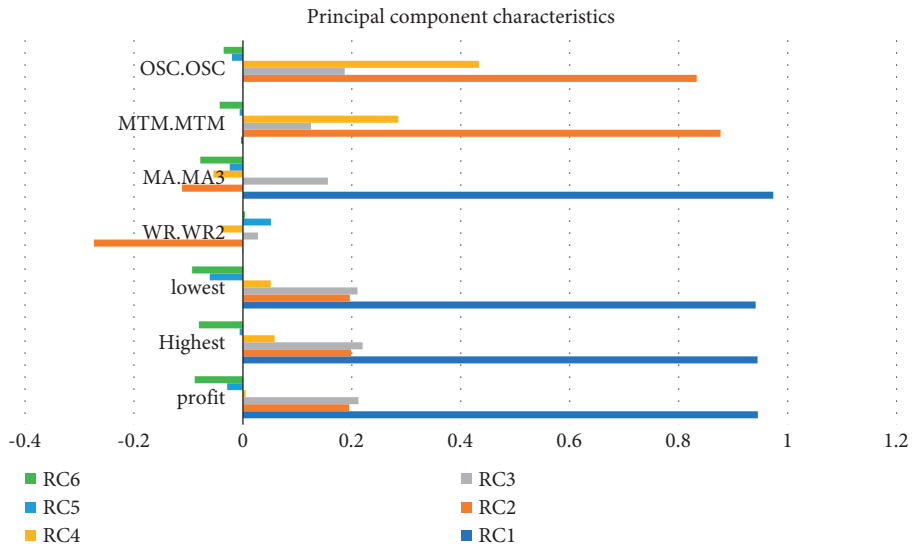

Figure 3: Principal component feature analysis.

Table 2: Main component evaluation index.

	RC1	RC2	RC3	RC4	RC5	RC6
CP	0.1535	0.3535	0.7474	−0.0868	0.1219	−0.0184
CR	0.2483	0.5096	0.536	0.4017	−0.256	−0.0933
C–F1	0.2981	0.1999	0.689	0.0047	0.2559	−0.3346
EP	0.0071	−0.0265	−0.1641	0.2175	0.0069	−0.0051
ER	0.1411	0.4014	0.6578	0.1225	−0.294	0.1221
E–F1	0.1891	0.0036	0.9024	−0.0307	0.0437	0.0195
OP	0.3858	−0.2712	0.2265	0.0165	0.304	−0.5153
OR	0.129	0.4455	0.7093	−0.0163	−0.0791	0.1523
O–F1	0.3228	0.0114	0.0387	0.011	−0.4751	−0.113
PCNT.PCNT	−0.0489	−0.0036	0.042	0.8405	−0.0144	−0.0023
PCNT.MAPCNT	−0.0476	0.4017	0.0211	0.8841	−0.0426	−0.018

Table 2: Continued.

	RC1	RC2	RC3	RC4	RC5	RC6
AMO.AMO2	0.4653	0.3189	0.4335	−0.0185	0.577	−0.022
VRSI.RSI3	−0.0397	0.4054	0.0615	0.3812	0.0391	0.2018
AMV.AMV2	0.9664	−0.0094	0.2118	−0.0614	−0.0229	−0.076
AMV.AMV3	0.978	−0.1596	−0.0036	−0.0347	0.0163	−0.0543
MCST.MCST	0.9613	−0.1087	−0.1285	−0.0628	0.0471	0.0148

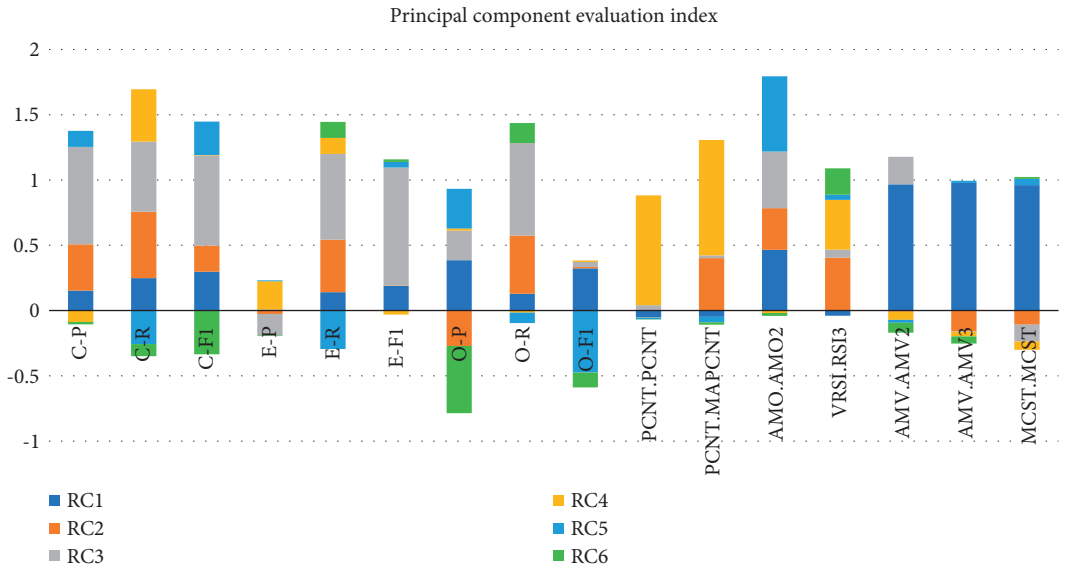

Figure 4: Principal component evaluation index.

Table 3: Time-dependent comparative experiment.

Time-dependent matrix type	CP	CR	C–F1	EP	ER	E–F1	OP	OR	O–F1
Directed + self	0.8611	0.9353	0.8967	0.8865	0.9506	0.9174	0.9956	0.9845	0.99
Directed	0.8381	0.8922	0.8643	0.8706	0.9468	0.9071	0.9939	0.983	0.9884
Undirected + self	0.6977	0.7759	0.7347	0.7826	0.7529	0.7674	0.991	0.9865	0.9888
Undirected time	0.6395	0.8103	0.7148	0.7309	0.692	0.7109	0.9974	0.9836	0.9904

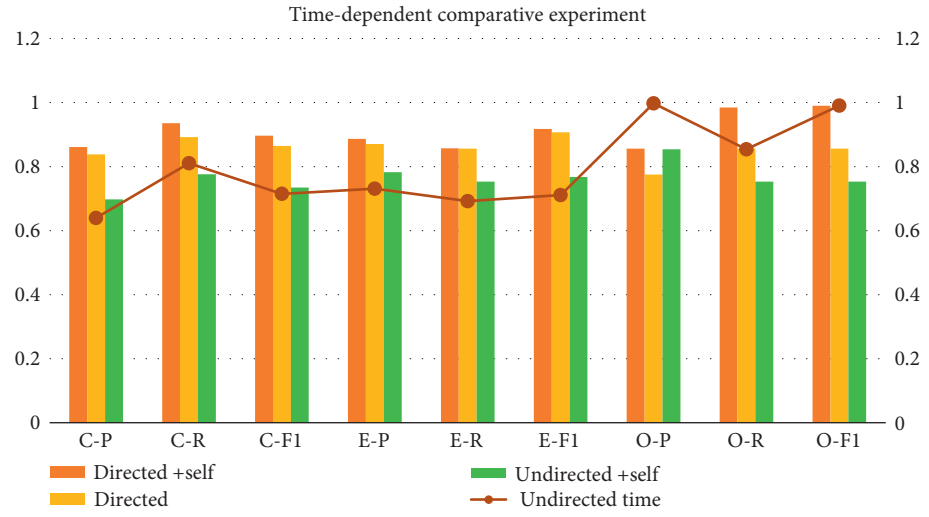

Figure 5: Time-dependent comparative experiment.

Table 4: Enterprise simulation experiment.

Time	Cost	Profit	Highest	Lowest	WR.WR1	WR.WR2	AMV.AMV2	AMV.AMV3	MCST.MCST
2020.01	30.78	30.11	30.1	29.7	81.21	45.62	32.67	34.95	36.08
2020.02	31.97	30.75	32.08	30.37	60.23	34.44	32.28	34.78	35.95
2020.03	31.56	31.97	32.2	31.4	31.23	24.62	31.96	34.69	35.88
2020.04	31.58	31.43	31.96	31.36	23.85	24.8	31.75	34.62	35.83
2020.05	31.92	31.58	32.56	31.38	21.62	22.38	31.46	34.5	35.73
2020.06	35.18	35.52	35.99	35.16	86.79	74.86	38.62	44.68	43.19
2020.07	35.16	35.84	35.86	35.13	87.09	75.43	38.04	44.61	43.05
2020.08	34.01	34.79	34.79	33.01	81.72	76.13	37.36	44.44	42.82
2020.09	34.1	34.47	34.78	34.07	79.2	73.99	36.86	44.3	42.7
2020.10	34.83	34.1	35.48	34	62	56.56	36.29	44.06	42.5

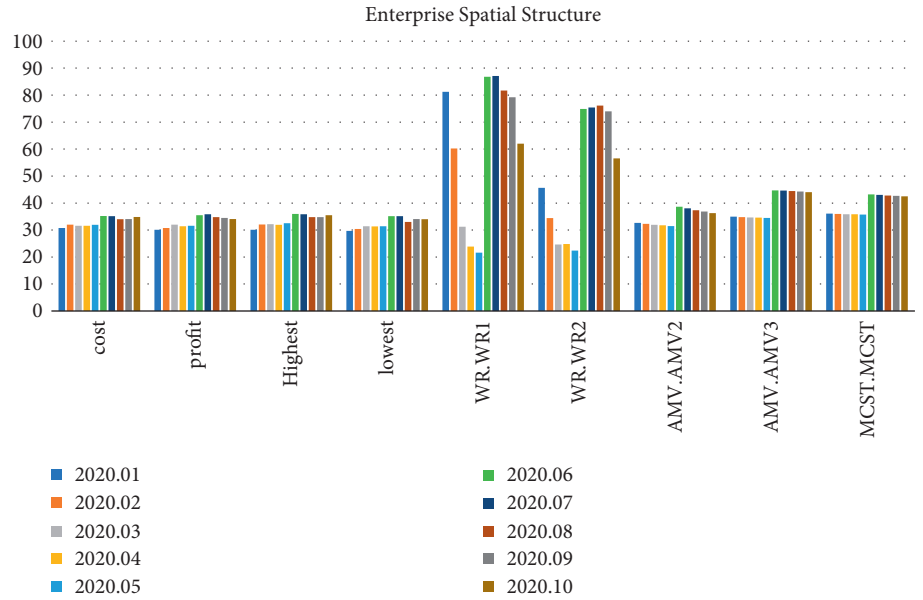

Figure 6: Enterprise simulation experiment.

Table 5: Enterprise economic forecast.

LSTM	BiLSTM	BiLSTM + GCN (dependency)	BiLSTM (WordNet)	BiLSTM + GAT	BLTGM (noNor)	BLTGM (nor)	BLTGM2	BLTGM3	MCST.MCST
−1.03	−1.1	−1.05	−1.09	−0.26	1.04	−0.17	−0.65	−0.61	−0.74
−0.9	−1.03	−0.95	−1.02	0.043	0.311	−1.59	−0.67	−0.63	−0.755
−0.95	−0.9	−0.94	−0.9	−0.5	−0.69	−0.89	−0.68	−0.64	−0.76
−0.94	−0.96	−0.96	−0.91	−0.79	−0.94	−0.89	−0.68	−0.65	−0.77
−0.96	−0.94	−0.9	−0.9	−0.07	−1.03	−0.97	−0.7	−0.67	−0.78
−0.68	−0.59	−0.66	−0.72	−0.18	1.06	0.87	0.45	0.4	0.17
−0.67	−0.62	−0.66	−0.6	−0.64	0.97	0.8	0.44	0.4	0.15
−0.59	−0.66	−0.59	−0.61	−0.16	0.37	0.2	0.41	0.39	0.13
−0.49	−0.62	−0.55	−0.56	0.21	−0.29	−1.46	0.37	0.39	0.09
−0.56	−0.49	−0.57	−0.52	−0.31	−0.01	−0.78	0.34	0.38	0.07

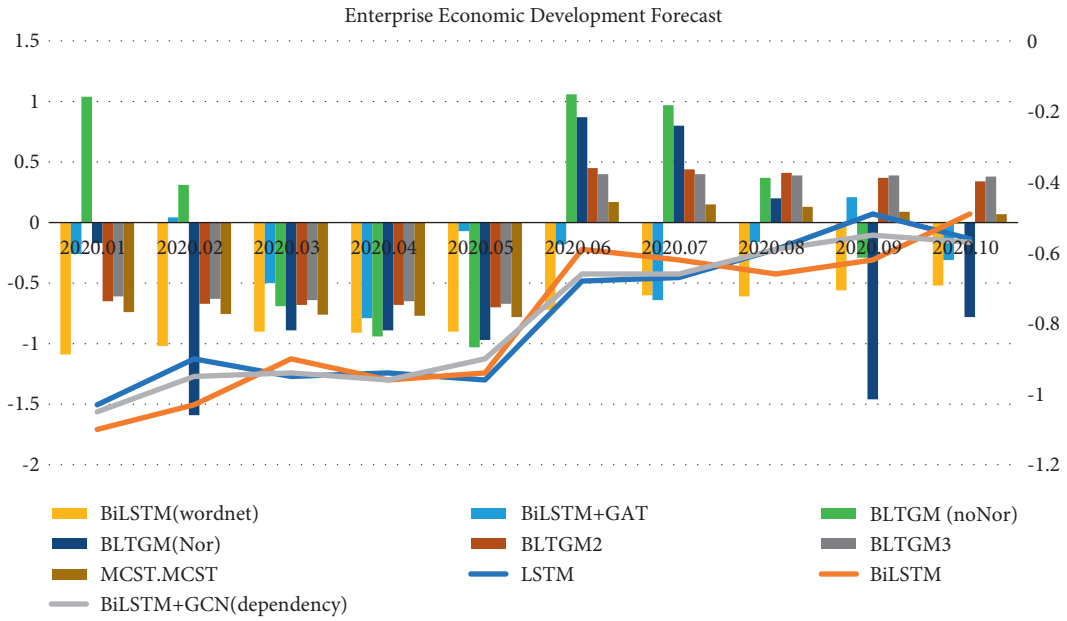

Figure 7: Enterprise economic forecast.

Table 6: Scores of different models.

Model	CP	CR	C–F1	EP	ER	E–F1	OP	OR	O–F1
LSTM	0.3829	0.3664	0.3744	0.3726	0.3004	0.3326	0.9155	0.9316	0.9234
BiLSTM	0.3648	0.3319	0.3392	0.4402	0.3916	0.4145	0.9215	0.9318	0.9266
BiLSTM + GCN (dependency)	0.3897	0.3578	0.373	0.4889	0.4183	0.4508	0.9247	0.9399	0.9322
BiLSTM (WordNet)	0.474	0.3922	0.4292	0.5	0.5209	0.5102	0.9355	0.9433	0.9394
BiLSTM + GAT	0.6882	0.8276	0.7515	0.7749	0.7985	0.7865	0.9997	0.9839	0.9917
BLTGM (noNor)	0.8375	0.8664	0.8517	0.8863	0.8593	0.8726	0.9853	0.9853	0.9853
BLTGM (Nor)	0.8611	0.9353	0.8967	0.8865	0.9506	0.9174	0.9956	0.9845	0.99
BLTGM2	0.8488	0.944	0.8939	0.9182	0.9392	0.9286	0.9951	0.9859	0.9905
BLTGM3	0.8065	0.9698	0.8806	0.9094	0.9544	0.9314	0.9994	0.9822	0.9907

Table 7: Principal component feature analysis of the LSTM model.

	RC1	RC2	RC3	RC4	RC5	RC6
SS loadings	8.63	6.91	5.21	3.84	2.25	2.18
Proportion var	0.23	0.19	14	0.1	0.06	0.06
Cumulative var	0.23	0.42	0.56	0.66	0.73	0.78
Proportion explained	0.3	0.24	0.18	0.13	0.08	0.08
Cumulative proportion	0.3	0.54	0.71	0.85	0.92	1

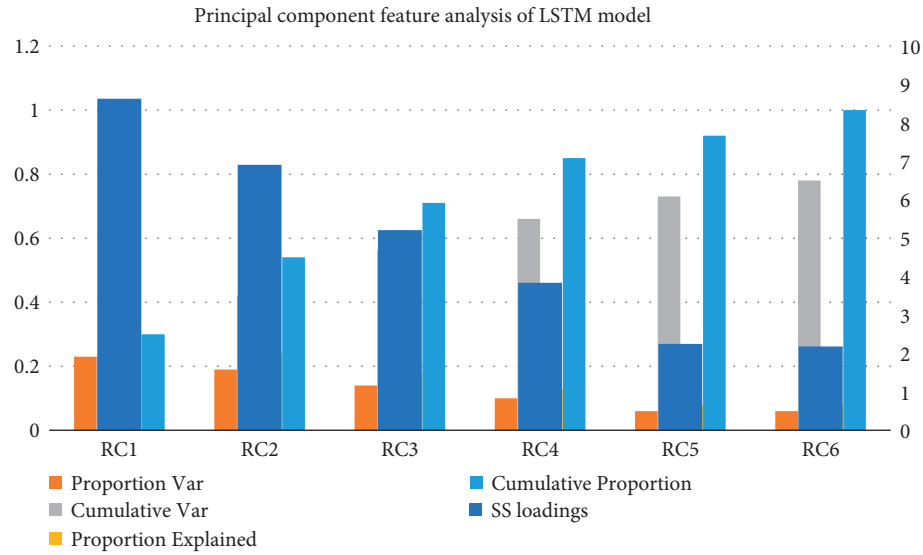

Figure 8: Principal component feature analysis of the LSTM model.

ER = 0.391, E–F1 = 0.4145, OP = 0.9215, OR = 0.9318, and O–F1 = 0.9266, as shown in Tables 6 and 7 and Figure 8.

Analyzing the principal component characteristics of LSTM, all data indicators meet the standards, and the best performance in the cumulative ratio is RC1 = 0.3, RC2 = 0.54, RC3 = 0.71, RC4 = 0.85, RC5 = 0.92, and RC6 = 1.

5. Conclusion

This study is based on the unsupervised learning-based enterprise spatial structure evolution and economic coupling coordination relationship situation assessment method. Pattern recognition has high-precision characteristics, but it is necessary to train the evaluation model for the enterprise spatial structure evolution in advance and then carry out economic coupling coordination based on the trained model.

Data Availability

The experimental data used to support the findings of this study are available from the corresponding author upon request.

Conflicts of Interest

The authors declare that they have no conflicts of interest regarding this work.

Acknowledgments

This work was supported by the Key Project of Chinese Ministry of Education of the 14th Five-Year Plan of the National Education Sciences Planning (DIA210365): Study on the Interactive Relationship between Spatial Structure of Local Enterprise and Supply of Talent in Local Colleges from the Perspective of Urban Transformation.

References

[1] M. Ochodek, S. Kopczyńska, and M. Staron, "Deep learning model for end-to-end approximation of COSMIC functional size based on use-case names," *Information and Software Technology*, vol. 123, Article ID 106310, 2020.

[2] Z. Zhuang, G. Liu, and W. Ding, "Cardiac VFM visualization and analysis based on YOLO deep learning model and modified 2D continuity equation," *Computerized Medical Imaging and Graphics*, vol. 82, Article ID 101732, 2020.

[3] G. Chen, Q. Pei, and M. M. Kamruzzaman, "Remote sensing image quality evaluation based on deep support value learning networks," *Signal Processing: Image Communication*, vol. 83, Article ID 115783, 2020.

[4] L. Carvelli, O. An, A. Brink-Kjær, E. B. Leary, and P. Jennum, "Design of a deep learning model for automatic scoring of periodic and non-periodic leg movements during sleep validated against multiple human experts," *Sleep Medicine*, vol. 69, pp. 109–119, 2020.

[5] Z. Song, T. Liu, and L. Shi, "The deep learning model combining CT image and clinicopathological information for predicting ALK fusion status and response to ALK-TKI therapy in non-small cell lung cancer patients," *European Journal of Nuclear Medicine and Molecular Imaging*, vol. 48, no. 2, pp. 361–371, 2021.

[6] G. Chen and S. Li, "Network on chip for enterprise information management and integration in intelligent physical systems," *Enterprise Information Systems*, vol. 15, no. 7, pp. 935–950, 2021.

[7] R. Ghosh, "A Recurrent Neural Network based deep learning model for offline signature verification and recognition system," *Expert Systems with Applications*, vol. 168, no. 5, 2020.

[8] F. M. Howard, J. Dolezal, S. Kochanny, J. Schulte, and A. T. Pearson, "The impact of site-specific digital histology signatures on deep learning model accuracy and bias," *Nature Communications*, vol. 12, no. 1, 2021.

[9] F. Niemeyer, F. Galbusera, Y. Tao, A. Kienle, and H. J. Wilke, "A deep learning model for the accurate and reliable classification of disc degeneration based on MRI data," *Investigative Radiology*, vol. 8, no. 12, pp. 61–71, 2020.

[10] J. Zaucha, C. A. Softley, M. Sattler, D. Frishman, and G. M. Popowicz, "Deep learning model predicts water interaction sites on the surface of proteins using limited-resolution data," *Chemical Communications*, vol. 56, 2020.

[11] E. Choi, S. Cho, and D. K. Kim, "Power demand forecasting using long short-term memory (LSTM) deep-learning model for monitoring energy sustainability," *Sustainability*, vol. 12, 2020.

[12] J. S. Raj, S. J. Shobana, I. V. Pustokhina, D. A. Pustokhin, and K. K. Shankar, "Optimal feature selection-based medical image classification using deep learning model in internet of medical things," *IEEE Access*, vol. 8, pp. 58006–58017, 2020.

[13] N. Shivsharan and S. Ganorkar, "Diabetic retinopathy detection using optimization assisted deep learning model: outlook on improved grey wolf algorithm," *International Journal of Image and Graphics*, vol. 21, Article ID 2150035, 2021.

[14] H. Shahabi, A. Shirzadi, S. Ronoud et al., "Flash flood susceptibility mapping using a novel deep learning model based on deep belief network, back propagation and genetic algorithm," *The Journal*, vol. 12, no. 3, p. 23, 2021.

[15] S. J. Im, N. D. Viet, and A. Jang, "Real-time monitoring of forward osmosis membrane fouling in wastewater reuse process performed with a deep learning model," *Chemosphere*, vol. 275, Article ID 130047, 2021.

[16] G. Foo, S. Kara, and M. Pagnucco, "Screw detection for disassembly of electronic waste using reasoning and retraining of a deep learning model," *Procedia CIRP*, vol. 98, no. 8, pp. 666–671, 2021.

[17] L. Cong, W. Feng, Z. Yao, X. Zhou, and W. Xiao, "Deep learning model as a new trend in computer-aided diagnosis of tumor pathology for lung cancer," *Journal of Cancer*, vol. 11, no. 12, pp. 3615–3622, 2020.

[18] X. Pan, Z. Lu, H. Huang, M. Wang, and H. Chen, "Improving nowcasting of convective development by incorporating polarimetric radar variables into a deep learning model," *Geophysical Research Letters*, vol. 48, 2021.

[19] H. Tanyildizi, A. Engür, Y. Akbulut, and M. Ahin, "Deep learning model for estimating the mechanical properties of concrete containing silica fume exposed to high temperatures," *The Journal*, vol. 14, no. 6, p. 15, 2020.

[20] X. Yang, Y. Fu, Y. Lei, S. Tian, and T. Liu, "Deformable MRI-TRUS registration using biomechanically constrained deep learning model for tumor-targeted prostate brachytherapy," *International Journal of Radiation Oncology, Biology, Physics*, vol. 108, no. 3, p. e339, 2020.

[21] A. Muhammad, S. Hong, and J. M. Lee, "A multi-layer perceptron based deep learning model to quantify the energy potentials of a thin film a-Si PV system," *Energy Reports*, vol. 6, pp. 1331–1336, 2020.

[22] S. M. Chiu, Y. C. Chen, and C. Lee, "Estate price prediction system based on temporal and spatial features and lightweight deep learning model," *Applied Intelligence*, vol. 52, pp. 808–834, 2022.

[23] W. M. Alenazy and A. S. Alqahtani, "Gravitational search algorithm based optimized deep learning model with diverse set of features for facial expression recognition," *Journal of Ambient Intelligence and Humanized Computing*, vol. 12, no. 10, 2021.

[24] X. Ning, W. Li, B. Tang, and H. He, "BULDP: biomimetic uncorrelated locality discriminant projection for feature extraction in face recognition," *IEEE Transactions on Image Processing*, vol. 27, no. 5, pp. 2575–2586, 2018.

[25] A. Onan and S. Korukoğlu, "A feature selection model based on genetic rank aggregation for text sentiment classification," *Journal of Information Science*, vol. 43, no. 1, pp. 25–38, 2017.

[26] S. K. AytuğOnana and H. Bulut, "Ensemble of keyword extraction methods and classifiers in text classification," *Expert Systems with Applications*, vol. 57, pp. 232–247, 2016.